Modeling and numerical simulation of nanosecond laser ablation

Mohamed-Rabie GUECHI[1*], Said ABBOUDI[2]

[1,2]ICB UMR 6303, CNRS, Univ. Bourgogne Franche Comte, UTBM
Department COMM, F-90010, Belfort, France.
[*](mohamed.guechi@utbm.fr)

Abstract- In this paper, the interaction of laser beam with a target and the evaporated material is studied theoretically. The target is ablated by a Nd:YAG laser pulsed working at its fundamental wavelength of 1064 nm with 80 ns pulse duration, the ablation is thermal and therefore the interaction of the laser beam with a target is studied with the use of thermal model and a hydrodynamic model. The model which describes both the target heating, formation of the plasma and its expansion consists of equations of conservation of mass, momentum and energy and is solved with the use of Fluent software package.

Keywords: laser ablation; plasma; CFD; iron; iron oxide.

Nomenclature

L_v	latent heat of vaporization, kJ/kg
L_m	latent heat of melting, kJ/kg
M	molar mass, kg/mol
R	universal gas constant, J/K.mol

Greek symbols

δ_a	depth of absorption, nm
δ_{th}	thermal penetration depth in the target solid, µm

Index and exponent

l	liquid phase
s	solid phase
v	vapor phase

1. Introduction

Examples of operations using high power laser sources are the surface treatment, these processing are intended to create surfaces that meet specific technological characteristics. This function is achieved by the removal or movement of material following a succession of laser impacts or the insertion of light elements in the surrounding atmosphere during the interaction. The purpose of laser surface treatment studies is to improve the mechanical (including hardness) and chemical (including corrosion resistance) characteristics of parts. The mastery of these processes requires understanding the different physical phenomena generated by the laser-material interaction. The impact of the laser beam on the surface of the target induces melting and rapid evaporation of the material. Once the critical value of the laser irradiance is reached, a breakdown occurs in the gas above the surface, leading to the formation of a plasma. This plasma absorbs a large amount of the laser radiation, it becomes very hot, and propagates in the direction of the laser beam with a very high speed. Laser ablation is a complex phenomenon that involves multiple physical processes that are both simultaneous and coupled. The methods of laser ablation are performed using laser pulses of duration of 10^{-9} – 10^{-7} s and irradiances of 10^6 – 10^{10} *W/cm²* these laser pulse parameters inevitably involve the formation of plasma above the processed material. The physical processes during laser ablation are: laser-target interaction, laser-plasma interaction, plasma expansion. In this study, a thermal model was used to simulate the laser - target interaction. For modeling plasma plume expansion, a fluid dynamics model is the most appropriate approach for modeling the laser ablation plume plasma formed in air at

https://doi.org/10.25855/SFT2020-166

atmospheric pressure, a bibliographic search [1,2]. The physical processes involved in laser ablation are the heat transfer in the target, the melting and vaporization of the material, the contribution of the Knudsen layer, the formation and expansion of the plasma, a rapid transformation through the liquid and vapor phases induced by laser-solid interactions is described by the thermal model with the Clausius-Claperyon equation to determine the vaporization temperature under different surface pressure conditions. The hydrodynamic behavior of steam during and after ablation is described by the gas dynamics equations (fluid dynamics).

2. Mathematical Model

To describe the interaction between the laser beam and the target during the ablation process laser, a thermal model has been developed. It is a 2D axisymmetric model, where the axis of symmetry corresponds to that of the laser beam. The macroscopic approach used in this model is justified by the fact that the laser pulse is of the order of a few nanoseconds and that the ablation is carried out on metals. In this case, the laser radiation is absorbed by free electrons present in metal, As the time of relaxation of energy in metals is of the order of 10^{-13} s [3], we can consider that in the case of the nanosecond laser pulse the energy of the laser radiation is instantly transformed into heat. The thermal model approximately agrees with experimental data on nanosecond laser ablation at moderate intensities of several W/m² (10^{10} – 10^{12} *W/m²*).

2.1. Laser – Target Interaction

The physical processes induced during the laser-target interaction are mainly influenced by the parameters of the laser beam (pulse duration, wavelength, irradiance) as well as by the physical properties of the treated materials, such as thermal diffusivity, latent heat of fusion and vaporization, the laser irradiation absorption factor. When interacting with a nanosecond laser beam with metal targets, a energy portion of the laser beam is reflected from the targets surface, while the other part is absorbed to a small depth, called the depth of penetration δ_a of the material which is on the order in nanometers. This effect is considered in the model. The energy of the beam laser absorbed by the target is then transformed into heat and transferred by conduction inside the material to a depth called the depth of thermal diffusion δ_{th} whiçh is on the order in micrometers ($\delta_{th} > \delta_a$). This magnitude, as well as the rate of heat transfer in the target depends the thermal diffusivity coefficient of the material. In most models, the heat transfer in the target is described by the 1D conduction heat transfer equation where the laser beam heat source ($I_{abs} = \alpha I_0$) is represented as a surface heat condition, α is the absorption coefficient of laser radiation, I_0 is the laser intensity.

2.1.1. Target Heating

An enthalpy-porosity technique [4,5], is used in Fluent for modeling the solidification/melting process. In this technique, the melt interface solid-liquid is not tracked explicitly. Instead, a quantity called the liquid fraction, which indicates the fraction of the cell volume that is in liquid form, is associated with each cell in the domain. The liquid fraction is computed at each iteration, based on an enthalpy balance. The mushy zone is a region in which the liquid fraction lies between 0 and 1. The mushy zone is modeled as a "pseudo" porous medium in which the porosity decreases from 1 to 0 as the material solidifies. When the material has fully solidified in a cell, the porosity becomes zero and hence the velocities also drop to zero [6]. For solidification/melting problems, the energy equation is written as:

$$\frac{\partial}{\partial t}(\rho H) + \nabla.(\rho \mathbf{v} H) = \nabla.(k \nabla T) + S \quad (1)$$

where H is the enthalpy, ρ is the density, **v** is the fluid velocity **v** = v_c + u, where v_c is the convection velocity and u is the recession velocity (Eq.2) and S is the surface heat source (the laser heating source term) , the enthalpy of the material is computed as the sum of the sensible enthalpy h and the latent heat ΔH, $H = h + \Delta H$ with : $h = h_{réf} + \int_{T_{réf}}^{T} c_p dT$ and the latent heat, $\Delta H = \sigma L_m$ [7], where L_m is the latent heat of melting and the liquid fraction σ.

- Solid–Liquid Mushy Zone - The heat diffusion Eq.1 is used with the boundary conditions, except at the solid and solid–liquid mushy zone boundary, the temperature is understood to be the melting temperature T_m.
At the solid and solid–liquid mushy zone boundary, the fraction of liquid is 0.
$\sigma = 0$ *at solid and solid − liquid mushy zone interface*
At the liquid and solid–liquid mushy zone boundary, the fraction of liquid is 1.
$\sigma = 1$ *at liquid and solid − liquid mushy zone interface*

- Liquid phase - Initially the liquid phase is at a uniform temperature, which is the melting temperature T_m. Therefore, the initial condition is:
$T_l(r,t) = T_m$ at $t = t_{sl}$, where t_{sl} is the time at which the solid–liquid mushy zone starts converting into the liquid phase.

- Initiation of Evaporation - Three phases exist as well as two mushy zones. Five differential equations are to be solved, one in each region along with the appropriate initial and boundary conditions. Again, it should be stated that liquid–vapor mushy zone and the vapor region move with time so that before calculating the quality and temperature in these regions respectively, their boundaries should be calculated according to the following criterion:
$T_l(r,t) \geq T_b \rightarrow$ *Liquid − vapor mushy zone, the fraction of vapor* $\geq 1 \rightarrow$ *vapor region,* where $T_l(r,t)$ is the liquid temperature and T_b is the boiling temperature.

- Liquid–Vapor Mushy Zone - In the liquid phase, Eq.1 is used with appropriate boundary conditions, except at the liquid and solid–liquid mushy zone boundary the temperature is taken to be the melting temperature.
At the liquid and liquid–vapor mushy zone boundary, the fraction of vapor phase is 0.
$\rho_l u(t) = 0$ *at liquid and liquid − vapor mushy zone interface*
At the vapor and liquid–vapor mushy zone boundary, the fraction of vapor phase is 1.
$\rho_l u(t) = 1$ *at vapor and liquid − vapor mushy zone interface.*

The vaporization rate $\rho_l u(t)$ is defined under the assumption that the flow of vaporized material from the surface follows the Hertz–Knudsen equation and the vapor pressure above the vaporized surface can be estimated with the Clausius–Clapeyron equation [8]:

$$u(t) = (1-\beta)\frac{\rho_b}{\rho_l}\sqrt{\frac{m}{2\pi k_B T_s}}.e^{\left(\frac{L_v}{k_B}\left(\frac{1}{T_b}-\frac{1}{T_s}\right)\right)} \quad (2)$$

where k_B is the Boltzmann constant, T_s is the surface temperature, T_b is the boiling temperature under a reference pressure p_b, and β is the fraction of the vaporized particles returning to the target surface (back flux). For stationary vaporization β = 0,18.

2.2. Laser – Plasma Interaction & Knudsen Layer

When ablated with a high-power laser beam, rapid vaporization occurs on the surface of the treated material. This rapid vaporization occurs when the absorbed energy density is much greater than the amount of energy required to vaporize the treated material. There is a model in

the literature [9,10], that treats the Knudsen layer as a hydrodynamic discontinuity (by introducing jump conditions to express the mass, momentum and energy balance). In the case of very high laser irradiance and at atmospheric pressure, the Mach number of the vapor reaches very quickly the value of 1, then, we consider that under the conditions studied, the vaporization of the material in the ambient atmosphere is in sonic mode of which parameters are:

$P_v = 0{,}21P_s$; $\rho_v = 0{,}31\rho_s$; $T_v = 0{,}67T_s$; $v_v = \sqrt{((0{,}67\gamma k_B T_v /m}$

where γ is adiabatic exponent, m is atomic mass. After plasma formation due to high laser irradiation, the plasma-plume that forms above the surface is strongly heated by the absorption of laser radiation until the end of the pulse, the energy of the laser radiation absorbed by the plasma-plume increases its internal energy, which leads to many processes of excitation and ionization, as well as a rapid increase in plasma species temperatures and densities.

2.3. Plasma Plume Expansion

The process of expansion of the plasma plume can also be described from a point of view macroscopic. The macroscopic approach greatly simplifies the hydrodynamic model. In our case, we study that the evolution of the macroscopic parameters of the fluid, that is to say the density of plasma and air, the velocity, the pressure and the temperature of the plasma. During laser ablation, the laser beam induces a breakdown in the metal vapor formed above the target and generates a plasma, which very quickly becomes opaque to laser radiation. This plasma, characterized by a very high temperature and pressure, extends with a supersonic velocity in the ambient atmosphere. This process can be considered as a rapid adiabatic expansion, which can be described by fluid dynamics. During its expansion, the plasma-plume compresses the surrounding gas thus generating a shock wave, which then continues its propagation in the ambient atmosphere. During the first few hundred nanoseconds after the start of the laser pulse, the plasma is so dense that it can be treated as a continuous fluid and the gas dynamics equations can be applied for its description. The plasma expansion model has been solved in axisymmetric with the use of the Ansys-Fluent software. The dynamic state of the metal vapor phase is described by the compressible and no dissipative Euler conservation equations for mass, momentum and energy [11-13].

2.3.1. Hydrodynamic Model - Macroscopic Approach

Mass conservation:

$$\frac{\partial}{\partial t}\rho + \nabla.(\rho \mathbf{v}) = 0 \tag{3}$$

Momentum conservation:

$$\frac{\partial}{\partial t}(\rho \mathbf{v}) + \nabla.(\rho \mathbf{v}\mathbf{v}) = -\nabla P \tag{4}$$

Energy conservation:

$$\frac{\partial}{\partial t}(\rho \boldsymbol{E}) + \nabla.(\mathbf{v}(\rho \boldsymbol{E} + p) = \alpha I_0 \tag{5}$$

where $\boldsymbol{E}$ is the total energy, $E = h - p/\rho + 0{,}5\ \mathbf{v}^2$, ρ *is the density,* $\rho = \frac{M}{R\ T}p$

3. Numerical Model of a Single Pulse

For modelling a laser ablation operation, one approach consists to assume the heating of the laser by means of a surface heat source, which is spatially and temporally distributed in the workpiece. The magnitude of the surface heat source depends on the laser surface intensity, the laser beam absorption depth, the thermal diffusion depth and the reflectance of the laser beam from the surface. Let us now list the major assumptions of the mathematical model employed in the analysis:

• The heat transfer problem is assumed to be 2D.
• Laser absorption is modelled by a surface heat source in the metal.
• Material has a certain absorption depth for the laser radiation.
• Laser beam intensity has Gaussian distribution.
• The material is a pure substance with single melting and evaporation temperatures.
• The vapor interacts with the laser beam, formation of a layer of Knudsen,
• Solid and liquid phases have the same absorption coefficient.

The computed steady state velocity and temperature fields during laser irradiation of iron Fe and iron (III) oxide Fe_2O_3 are presented in Fig.1. During laser irradiation, the rise and decay of the peak temperature at the surface of a metal can be determined analytical [14], results from analysis of uniform rate heating of semi-infinite slab, where the heated layer thickness δ_{th} is given by: $\delta_{th} = 0{,}969\sqrt{\kappa.\tau}$ ~ 1.4 µm (for Fe) and 0.52 µm (for Fe_2O_3), where κ is the thermal diffusivity.
From the theoretical solution, the resulting surface temperature is:

$$\Delta T_{analytical} = \frac{2I_{abs}\sqrt{\tau}}{\sqrt{\pi k \rho C_p}} \quad (6)$$

where τ is the pulse laser, k is the thermal conductivity and C_p is the specific heat capacity. The boundary condition at the laser beam impact is, [9]:

$$-k\frac{\partial T_s}{\partial n} = \alpha I_0 - \rho_l u(t).L_v \quad (7)$$

Where I_0 is the laser intensity, α is the absorption coefficient, L_v is the latent heat of vaporization.

The boundary conditions used during the numerical simulations are presented on Fig.1.

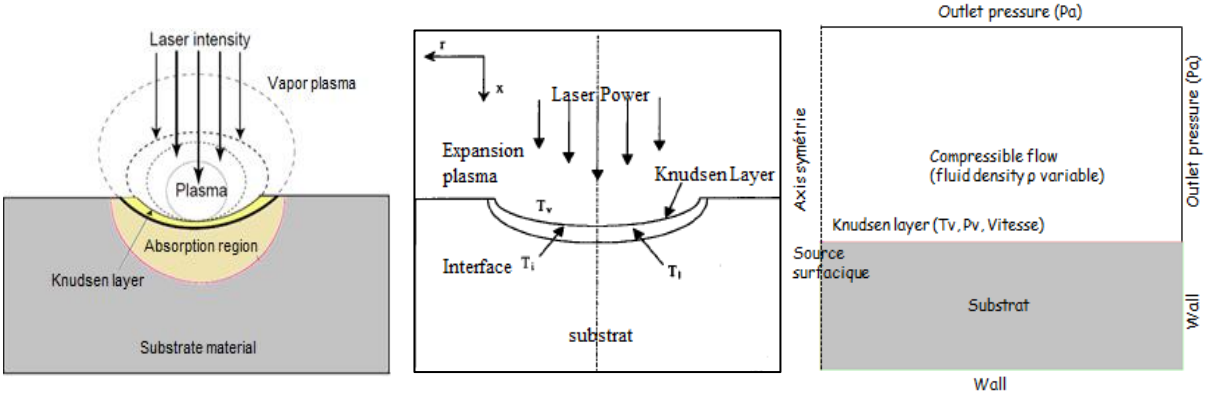

Figure 1: *Calculation Domain*

4. Results and discussions

4.1. Laser-target interaction simulation

The figures 2(a, b), shows the temperature contours in the two materials after 80 ns for the intensity laser of $2.5\text{x}10^{11}$ W/m², $8.3\text{x}10^{10}$ W/m², and $1.3\text{x}10^{12}$ W/m², $4.1\text{x}10^{11}$ W/m² respectively. According these figures, it is observed that the surface temperature of the target increases as a function of the laser power for the two studied materials (iron Fe, hematite Fe_2O_3). With the same pulse duration 80 ns, the temperature rise is observed on the target surface. Table 1 gives the comparison between the analytical (Eq.6) and the numerical methods for the

calculation of the elevation of the temperature at the surface of the materials. For the two powers used in this study, it is observed from the table1, that the comparison between the analytical and numerical results and gives a difference of order of 20° to 900° in the case of hematite (Fe_2O_3) and 26° to 100° in the case of Iron (Fe), with a percentage quite low. It can be seen that the temperature drops quickly to room temperature at a distance of about one time the beam radius away from the cavity center with a larger gradient close to the cavity surface.

P_u = 20 W	$\Delta T_{analytical}$ (°)	$\Delta T_{numerical}$ (°)	Diff (°)	%
Fe	$5{,}84.10^3$	$5{,}86.10^3$	26	0,44
Fe_2O_3	$3{,}73.10^3$	$3{,}75.10^3$	20	0,53
P_u = 100 W	$\Delta T_{analytical}$ (°)	$\Delta T_{numerical}$ (°)	Diff (°)	%
Fe	$2{,}92.10^4$	$2{,}93.10^4$	100	0,34
Fe_2O_3	$1{,}9.10^4$	$1{,}99.10^4$	900	4,70

Table 1: *The comparison between the analytical and numerical results*

4.2. Interaction laser-cible / Knudsen layer

During the LA (Laser Ablation) process of Fe, a crater with high-density plasma is formed. The dense plume expands, then, above the target surface pushing the ambient air gas away. The computational y-profiles of temperature and y component of velocity in the ns laser-ablated Iron plume expanding in background air at 1 atm are shown in Fig.3 for various time moments. we analyze the temporal behavior of temperature in the plume during its expansion. First, let us focus on the plume's center. During the first t = 80 ns, the plume expands less than 0.1 mm. A nearly stepwise temperature drops until to 2000K of the plasma is occurred. This decrease of the initial temperature is due to the intense heat transfer that exists between the hot plasma and cold air. The hot high-temperature region in the vicinity (velocity) of the plume's center at later expansion stages was previously reported in [13].

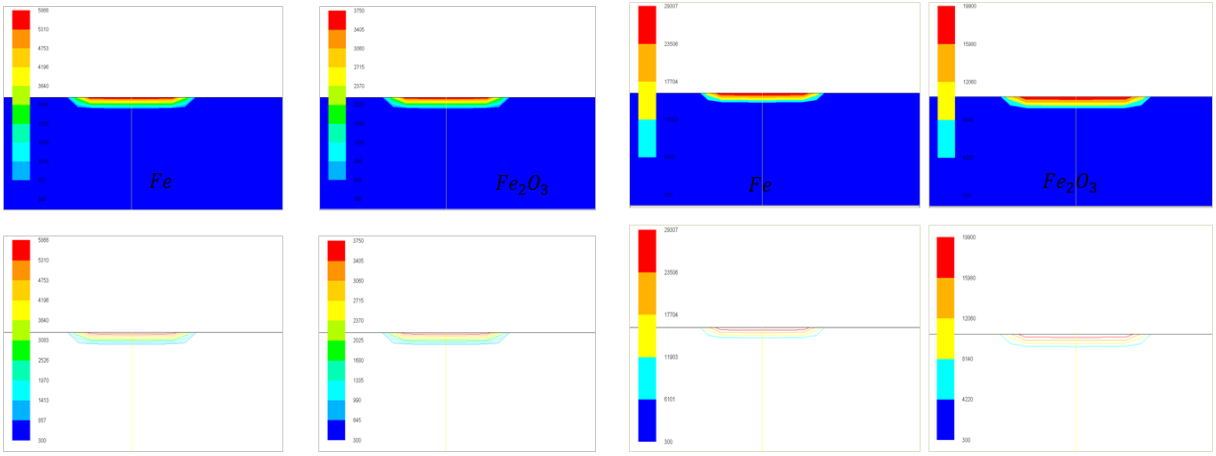

(a) (b)

Figure 2: *Temperature contours at the end of a 80 ns laser pulse.*
(a) I_{abs} = 2,5x10^{11} W/ m² (Fe), I_{abs} = 8,3x10^{10} W/ m² (Fe_2O_3)
(b) I_{abs} = 1,3x10^{12} W/ m² (Fe), I_{abs} = 4,1x10^{11} W/ m² (Fe_2O_3)
Wavelength λ = 1064 nm, *Gaussian beam, beam radius r = 27* μm,

The expansion of dense high-pressure Laser in background air at 1 atm generates strong shock waves at the interface between plasma and air. During the initial stage of expansion, the

plume impacts the ambient gas as a supersonic piston. The shock wave generated by more energetic nanosecond laser, pushes into the stationary air gas causing its compression to high density in a thin region Fig.3. As a result, a large jump of mass density is observed at the shock wave front with a low-density region formed behind it. The expansion of the plasma plume is achieved due to transformation of thermal energy into kinetic energy with resultant drop in temperature and pressure. Consequently, the plume's front of the expanding plasma acquires a supersonic velocity in a very short time, the plasma hot core is located near the surface where laser energy release takes place with the local temperature maximum at the forefront, Fig.3. However, the temperature of the plume's center remains much higher compared to that at the shock wave front.

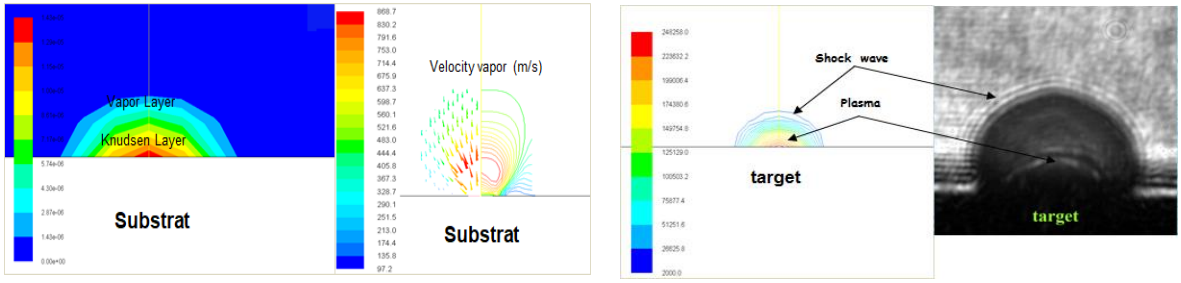

Figure 3: *Distribution of temperature and velocity at the level Knudsen layer and formation of plasma*

4.3. Plasma expansion

Contour plots of 2D density and velocity distributions taken at t ~ 80 ns and t ~1 μs are presented in Fig.4. It is found that radial expansion of the plume is rather limited at this instant. The instant 70 ns, corresponds to steady expansion regime that is characterized by the axial expansion velocity being two times as high as the radial one. The density distribution is characterized by a rapid decrease with the distance from the surface target. Starting from the Knudsen layer, the density begins to decrease from the target surface until the value almost zero, and the mass density of plasma near the plume's center decreases further. It is seen in Fig.4, that the flow of plasma is directed outwards from a crater and the velocity is small in the vicinity of the plume's center. At the shock front, the plasma velocity in the y-direction is much higher than that in the x-direction and at t ~ 100 ns, it is still higher. In the vicinity of the plume's center, the vortex starts to develop. At t ~1μs, the shock front of the nanoseconds plume continues to have a higher velocity in the y-direction. However, the difference in the magnitude of velocities decreases along the two directions.

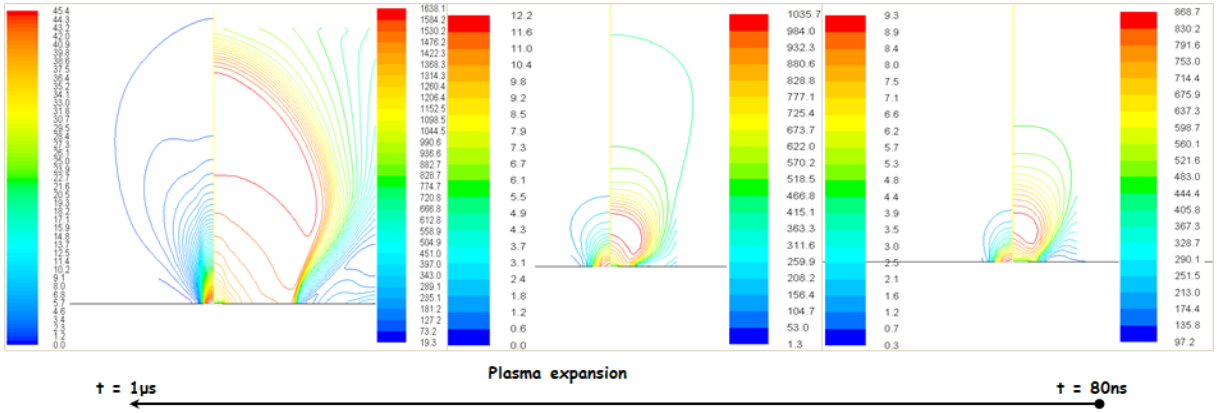

Figure 4: *Distribution of density and velocity in plasma induced during laser ablation of Iron, after the beginning of the laser pulse*

5. Conclusion

The model which describes the target heating, the plasma formation and the plasma expansion is governed by the conservation equations system of mass, momentum and energy and is solved with the use of commercially available program Fluent. The calculations show a sharp increase of the plume temperature and density as a result of plasma-laser beam interaction, and following it a considerable increase of the velocity of the plasma plume. The obtained numerical and the theoretical results are in fair agreement. The plume velocity obtained from the model is close to that observed in the experiment carried out in similar conditions; this means that high plume velocities observed in experiments can be fully explained by gas dynamic effects.

References

[1] K. R. Chen, J. N. Leboeuf, R. F. Wood, D. B. Geohegan, J. M. Donato,C. L. Liu, A. A. Puretzky, Laser-solid interaction and dynamics of laser-ablated materials, *Applied Surface Science*, 96-98, (1996) 45-49.

[2] R. F. Wood, K. R. Chen, J. N. Leboeuf, A. A. Puretzky and D. B. Geohegan,Dynamics of plume propagation and splitting during pulsed-laser ablation, *Physical Review Letters*, 79 (8), (1997), 1571-1574.

[3] M. Von Allmen, Laser Beam Interactions with Materials, (*Springer, Heidelberg*, 1987).

[4] V. R. Voller and C. Prakash. "A Fixed-Grid Numerical Modeling Methodology for Convection-Diffusion Mushy Region Phase-Change Problems". *Int. J. Heat Mass Transfer*, 30 (1987),1709–1720.

[5] V. R. Voller. "Modeling Solidification Processes". *Technical report. Mathematical Modeling of Metals Processing Operations Conference*, Palm Desert, CA American Metallurgical Society. 1987.

[6] Fluent, "Users Guide," vol. Vol 1,2 &3, pp. 2005.

[7] M. A Sheikh, Modelling & simulation of laser material processing: predicting melt pool geometry and temperature distribution, *Proceeding of International Conference MS'07, India*, (2007) 3-5.

[8] N.M. Bulgakova, A. Bulgakov, L.P. Babich, Energy balance of pulsed laser ablation: thermal model revised, *Appl. Phys. A*, 79, (2004), 1323–1326.

[9] Knight, C. J., 1979, "Theoretical Modelling of Rapid Surface Vaporization with Back Pressure", *AIAA Journal*, 17(1979), 519-523.

[10] T. Mościcki, J. Chrzanowska, Hydrodynamic model of nanosecond laser ablation of tungsten and boron, *Conference on Modelling Fluid Flow (CMFF'15), Budapest, Hungary, September* 2015, 1- 4.

[11] C P. Grigoropoulos, T D. Bennett, J-R. Ho, X. Xu, and X. Zhang, « Heat and Mass Transfer in Pulsed-Laser-Induced Phase Transformations », *Advances in heat transfer*, 28, 75-144.

[12] T. Mościcki, J. Hoffman, Z. Szymański, 'Modelling of plasma formation during nanosecond laser ablation' *Arch. Mech. Warszawa*, 63, 2 (2011), 99–116.

[13] A.V. Bulgakov and N.M. Bulgakova, Dynamics of laser-induced plume expansion into an ambient gas during film deposition, Journal of Physics D: *Applied Physics* 28(8) (1995), 1710-1718.

[14] H. S. Carslaw and J. C. Jaegar, Conduction of Heat in Solids, *Oxford University Press, Oxford*, 1959.